Two-Color Two-Dimensional Electronic Spectroscopy Using Dual Acousto-Optic Pulse Shapers for Complete Amplitude, Phase, and Polarization Control of Femtosecond Laser Pulses

ARTICLE *in* THE JOURNAL OF PHYSICAL CHEMISTRY A · APRIL 2013

Impact Factor: 2.69 · DOI: 10.1021/jp400603r · Source: PubMed

7 AUTHORS, INCLUDING:

Pooja Tyagi
Massachusetts Institute of Technology
14 PUBLICATIONS **190** CITATIONS
SEE PROFILE

Jonathan I Saari
ETH Zurich
13 PUBLICATIONS **157** CITATIONS
SEE PROFILE

Nicolas Forget
Fastlite
108 PUBLICATIONS **704** CITATIONS
SEE PROFILE

Patanjali Kambhampati
McGill University
61 PUBLICATIONS **3,104** CITATIONS
SEE PROFILE

THE JOURNAL OF PHYSICAL CHEMISTRY A

Article

pubs.acs.org/JPCA

Two-Color Two-Dimensional Electronic Spectroscopy Using Dual Acousto-Optic Pulse Shapers for Complete Amplitude, Phase, and Polarization Control of Femtosecond Laser Pulses

Pooja Tyagi,[†,§] Jonathan I. Saari,[†,§] Brenna Walsh,[†] Amin Kabir,[†] Vincent Crozatier,[‡] Nicolas Forget,[‡] and Patanjali Kambhampati*[,†]

[†]Department of Chemistry, McGill University, Montreal, Quebec H3A 0B8, Canada

[‡]Fastlite, Centre scientifique d'Orsay - Bât.503, Plateau du Moulon - BP 45, Orsay, France

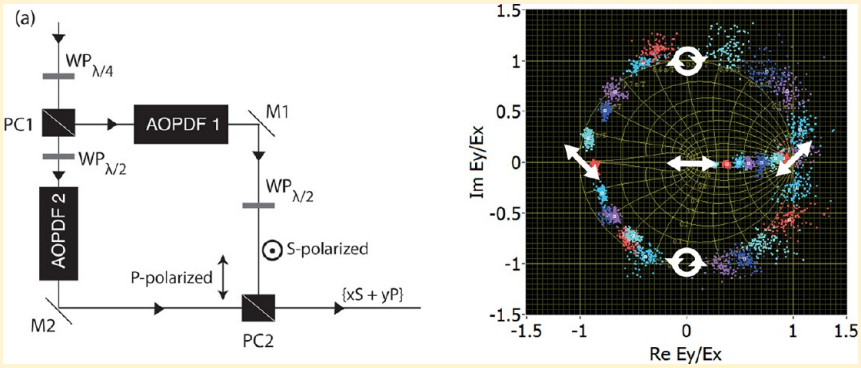

ABSTRACT: We demonstrate a dual pulse-shaper setup capable of independent polarization, phase, and amplitude control over each pulse. By using active phase stabilization, we achieve a phase stability of ~λ/314 between the two pulse shapers, making the dual-shaper setup suitable for both two-quantum and one-quantum measurements. The setup is compact and easily switchable between pump−probe and collinear geometries. We further illustrate the functionality of the dual-shaper setup by performing two-color 2D visible spectroscopy on colloidal CdSe quantum dots in pump−probe geometry.

1. INTRODUCTION

Two-dimensional spectroscopy has emerged as a powerful tool that can determine the complete nonlinear optical response of a system up to third-order. By providing access to specific quantum mechanical pathways, it allows for the measurement of vibrational and electronic couplings, energy transfer, and multiexciton correlations, among other observables.[1−6] Two-dimensional experiments can be implemented in different beam geometries, each having its advantages. For example, the boxcar geometry offers background-free detection, thereby eliminating the need for phase cycling.[7,8] The collinear geometry, desirable for its simplicity, is easy to extend to higher-order experiments and allows for both fluorescence and transmission detected experiments.[9,10] The pump−probe geometry has the advantage of directly measuring perfectly phased 2D spectra as it emits both rephasing and nonrephasing components in the same direction.[11−13]

Traditionally, the pump−probe configuration employs a single pulse shaper to generate a phase-coherent pump pulse pair, and the probe pulse, which also acts as the local oscillator, is derived from a second source such as a white light continuum or a noncollinear OPA.[11,12,14] This configuration works well for one-quantum (1Q) measurements where the pump and the probe pulses are not required to be phase-coherent with each other. However, in the case of two-quantum (2Q) measurements, all optical pulses need to be phase-coherent, which presents a challenge when using separate laser sources to produce pump and probe pulses.[4] Additionally, a single pulse shaper cannot independently control the polarization of each pump pulse; therefore, the polarization of the pump pulses must be identical. This restriction does not allow the use of optimal polarization selective schemes to completely eliminate the background because they require the polarizations of the two pump pulses to be orthogonal.[15]

We overcome these limitations by using dual pulse shapers (acousto-optic programmable dispersive filters (AOPDFs): WR25, low-jitter operation), which enable independent polarization, phase, and amplitude control over each pulse (Figure 1). In this configuration, we can achieve a phase stability of ~λ/314 between the two shapers by using active phase stabilization. In addition to being extremely compact, this setup is easily switchable between pump−probe and collinear geometries, allowing for detection in both phase-cycling and phase-matching arrangements (Figure 1). Fast update rates of the

Special Issue: Prof. John C. Wright Festschrift

Received: January 18, 2013
Revised: March 18, 2013
Published: April 18, 2013

   dx.doi.org/10.1021/jp400603r | J. Phys. Chem. A 2013, 117, 6264−6269

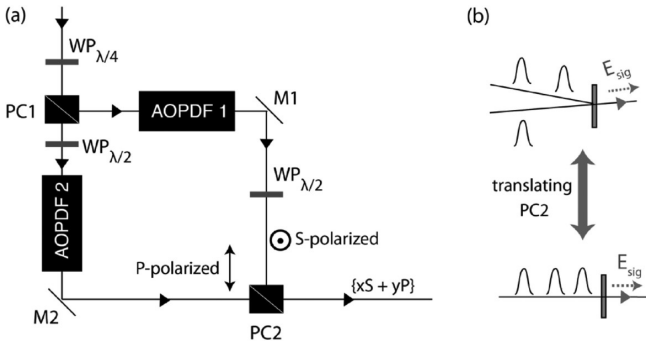

Figure 1. (a) Outputs of the two OPAs are orthogonally polarized and are separated using a polarizing cube (PC1). Each polarization component is then sent through an AOPDF to produce shaped pulses, which are finally combined using PC2. (b) Translating PC2 spatially separates the shaped pulses from the two AOPDFs, making it easy to switch between the pump–probe (top) and collinear (bottom) geometries.

AOPDF enable single-shot measurements at 1 kHz, significantly reducing the data acquisition time. Also, we compress the unshaped pump pulse before the shaping setup using prism compressors; this compensates for part of the dispersion of the AOPDFs and allows us to produce a delay of up to 4 ps between the shaped pulses. Finally, we demonstrate the functionality of the dual pulse shaper setup by performing 2D visible spectroscopy on CdSe quantum dots (QDs).

2. EXPERIMENT

The ultrafast laser source used in these experiments is an amplified Ti-sapphire laser system (2.5 mJ, 70 fs, 800 nm, 1 kHz). The regenerative amplifier is used to pump two optical parametric amplifiers (OPAs), which were used to produce the pump and the probe pulses. A block diagram of our pulse shaping setup is shown in Figure 1a. The output of one OPA was sent to AOPDF 1, which produces the pump pulse pair (532 nm, 10 nm fwhm), and the other OPA was used to produce the probe pulse (616 nm, 25 nm fwhm), which was shaped by AOPDF 2.

In pump–probe geometry, the signal field is emitted in the same direction as the probe and is resolved at 1 kHz using the Acton SP2500i spectrometer and PIXIS 100B CCD. A color filter was used to block the pump pulses from reaching the detector. The instrument response function (IRF) was measured by cross-correlation between the pump and the probe pulses and was found to be ~60 fs. The coherence time (t_{coh}) was scanned from 0 to 200 fs in 0.4 fs time steps for a fixed population time (T_p). The energy of the pump and the probe pulses was 25 and 2.5 nJ, respectively. Samples of colloidal CdSe QDs dispersed in toluene were purchased from NN-Laboratories; the sample was continuously flowed through a 1 mm path length flow cell during the experiment. The optical density of the sample was ~0.2.

3. RESULTS

Previous experiments have shown that a pulse pair produced by single Dazzler pulse shaper can maintain a phase stability of ~λ/85 at 530 nm over 3 h.[12] However, a single Dazzler setup does not allow for 2Q measurements in pump–probe geometry and also lacks the ability to independently control the polarization of individual pump pulses. To overcome these limitations, we use two Dazzlers with active phase stabilization to achieve high phase stability between the pulse pair produced by them. Basically, a spectral interferogram between the two pulses is measured to determine their relative phase difference, and the required phase correction is applied in subsequent shots to achieve the target phase difference.

The phase stability measurements were performed using spectral interferometry. Figure 2 shows a comparison of the phase stability produced by single AOPDF without active phase stabilization and two AOPDFs with active phase stabilization at 100 Hz (i.e., using every 10th shot to determine the phase correction). In both cases, the shaped pulses had identical spectra and the measurements were made at 630 nm. Using active phase stabilization, we can produce a phase stability of ~λ/314 (at 630 nm over 1 h) between pulses produced from the two AOPDFs (Figure 2a), which is, to our knowledge, the highest reported phase stability to date for pulse pairs generated by AOPDFs. In fact, it surpasses the phase stability produced by a single AOPDF (Figure 2b). By maintaining excellent phase stability between two AOPDFs, this setup extends the application of pulse shapers to 2Q measurements.

Another important application of our setup is the ability to independently control the polarization of individual pump pulses at 1 kHz. This is accomplished by combining the pulses produced from the two shapers using a polarizing cube. Because the pulses shaped by the two AOPDFs have orthogonal

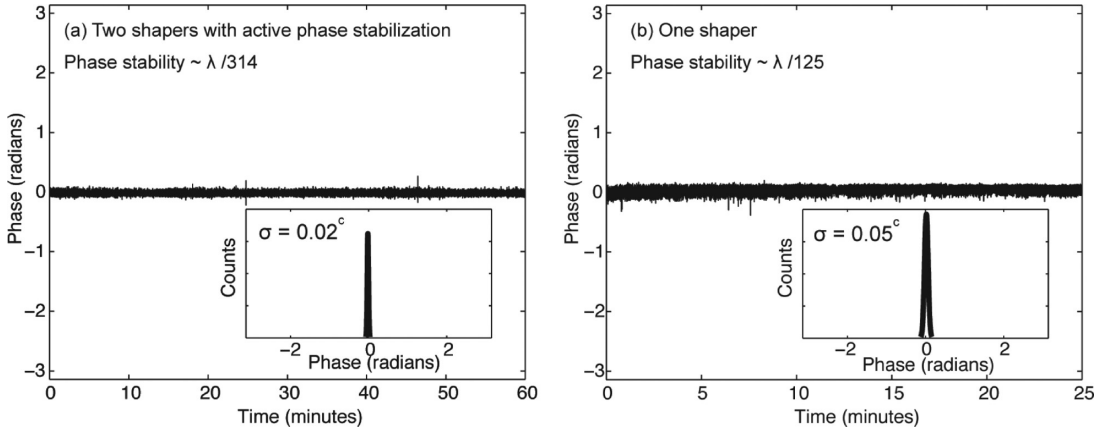

Figure 2. Single-shot (1 kHz) phase measurements (using spectral interferometry) between two pulses (a) from two AOPDFs using active phase stabilization at 100 Hz over a period of 60 min and (b) from a single AOPDF over a period of 25 min.

dx.doi.org/10.1021/jp400603r | J. Phys. Chem. A 2013, 117, 6264–6269

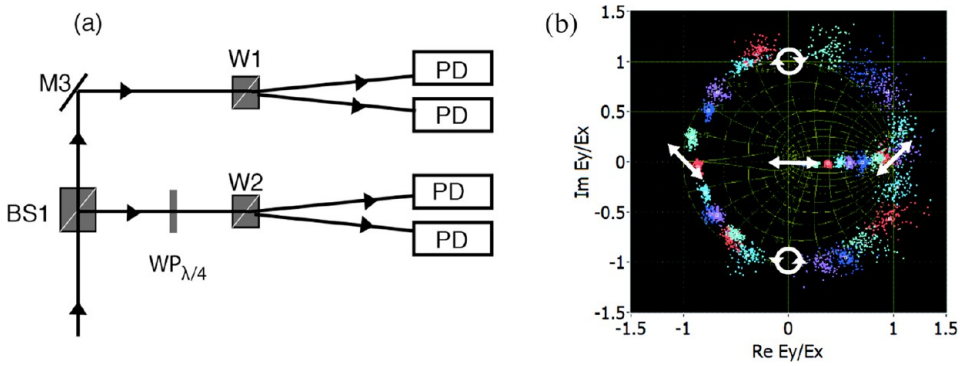

Figure 3. (a) Polarization characterization is achieved by splitting the shaped pulse using a beam splitter (BS1) and subsequently Wollaston prisms (W1, W2) and measuring the intensity of the circularly and linearly polarized components using photodiodes (PDs). (b) Polarization measurements using the ellipsometer shown in panel a. The data points are presented on a Poincaré sphere for easy visualization. 100 shots are acquired for each phase and amplitude setting. Both linearly and circularly polarized pulses can be produced using the shapers shown in Figure 1a.

polarizations (Figure 1a), by controlling the spectral phase and amplitude of each of these pulses, we can achieve any desired polarization state. Zanni and coworkers have successfully implemented this principle for polarization control in the mid-infrared (mid-IR).[16] They use a wire-grid polarizer for combining mid-IR pulses, whereas we use a polarizing cube (PC2) for the same purpose in the visible range. PC2 combines the pulses from the two AOPDFs while the feedback loop ensures high phase stability between the two Dazzlers, which is critical to achieve polarization shaping. The translation of PC2 controls the spatial overlap between the two pulses from the two Dazzlers, thereby allowing us to easily switch between collinear and pump−probe geometries. When the pulse pair is perfectly overlapped, collinear polarization shaped pulses are produced. However, when the pulse pair is spatially separated, we lose the ability to independently control the polarization of the individual pump pulses while still maintaining excellent phase stability between the two shapers necessary to perform 2Q experiments. This implies that when using Dazzlers for polarization shaping of individual pump pulses we can either (i) use a separate laser source for the probe pulse and perform the 2D experiments in pump−probe geometry or (ii) use the Dazzlers to shape both pump and probe pulses and perform the experiment in collinear geometry.

To characterize the pulse polarization, we employ a simplified Mueller ellipsometer shown in Figure 3a. The ellipsometer uses a beam splitter (BS1) and two Wollaston prisms (W1 and W2) to measure two quadratures of the polarization state in both linear and circular polarization bases, thus characterizing the polarization of the shaped pulses. Figure 3b presents the polarization measurements on a Poincaré sphere for easy visualization. By controlling the phase and amplitude of pulses from each AOPDF and combining them using PC2, we can prepare pulses in the desired polarization state. By varying $\Delta\phi$ from 0 to 2π (in steps of $\pi/10$), we obtain the data spanning the circumference of the Poincaré sphere. These data points correspond to polarization states of varying ellipticity, from right-handed to left-handed circular polarization. By varying the amplitude of one of the pulses from 0 to 1, we obtain data along the equator, which corresponds to linear polarization states.

Finally, we demonstrate the functionality of the dual AOPDF scheme for 2D visible spectroscopy by using colloidal CdSe QDs dispersed in toluene as a test sample. The experiments were performed in pump−probe geometry, with AOPDF 1 producing the pump pulse pair and AOPDF 2 producing the probe pulse. The pump pulses were tuned to the 1P exciton peak, while the probe pulse was set to 1S exciton (Figure 5a). The polarization of the probe pulse was set to 45° relative to the pump pulses. Because the signal field is emitted collinear to the probe pulse that acts as the local oscillator, an analyzer was used to block probe pulse before the detector by setting it at 85° relative to the probe pulse. This allows us to increase the probe intensity without saturating the detector, and the small amount of probe passing through the analyzer allows for heterodyne detection. This polarization scheme significantly enhances the signal-to-noise of the 2D spectrum by predominantly measuring (X+Y)(X+Y)XY = XYXY+YXXY components (where X and Y denote 0 and 90° polarizations, respectively).[12,15,17] A small contribution from (X+Y)(X+Y)XX = XXXX+YYXX is also present because the analyzer is not perfectly perpendicular to the probe polarization.

The desired 1Q 2D absorptive spectrum is the sum of the rephasing (R) and nonrephasing (NR) signals.[18] In the pump−probe configuration, both of these signals are emitted in the direction of the probe pulse. Thus, the detected signal in pump−probe geometry directly measures the 2D spectrum, unlike the noncollinear geometries where NR and R signals are emitted in different phase-matched directions and must be separately measured, phased, and added to obtain the 2D absorptive spectrum.[19] The disadvantage of the pump−probe geometry, however, is that it is not background-free. The unwanted transient absorption signals due to two light-matter interactions from single pump pulse and one from the probe pulse are also emitted in the probe direction. To eliminate the transient absorption background, we employ a two-step phase-cycling scheme introduced by Zanni and coworkers.[17] The phase of the emitted one-quantum signal is given by

$$\phi_{sig} = \pm(\phi_1 - \phi_2) + \phi_3 - \phi_{LO}$$

where, $\phi_{1(2)}$ is the phase of the first (second) pump pulse, ϕ_3 is the phase of the probe pulse, and ϕ_{LO} is the phase of the local oscillator pulse and ± signs refer to NR and R components, respectively. In pump−probe geometry, because the probe pulse acts as the local oscillator, that is, $\phi_3 = \phi_{LO}$, the phase of the NR and R signals is independent of ϕ_3 and is equal to $\pm(\phi_1 - \phi_2)$, respectively. From the discussion above, it follows that changing $\Delta\phi = (\phi_1 - \phi_2)$ by 'δ' changes the phase of the desired 2D signal by the 'δ' as well, while keeping the phase of the transient absorption signal unchanged. Therefore, subtract-

dx.doi.org/10.1021/jp400603r | J. Phys. Chem. A 2013, 117, 6264−6269

ing measured signals corresponding to $\Delta\phi = 0$ and $\Delta\phi = \pi$ will enhance the desired 2D signal while eliminating the transient absorption background. Figure 4 shows the detected signal as a

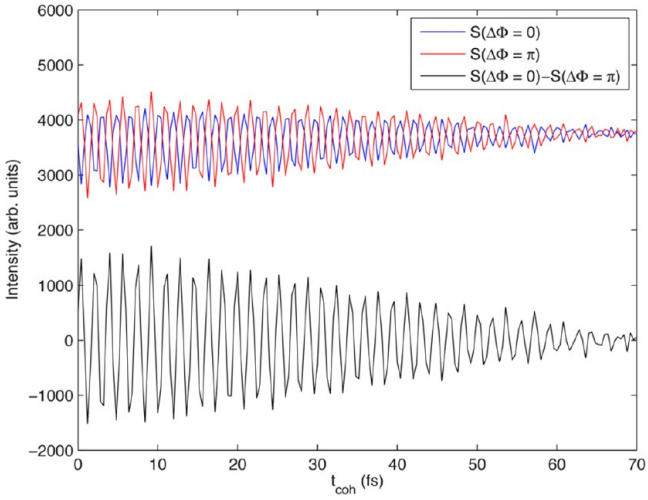

Figure 4. Demonstration of two-step phase-cycling scheme. The measured raw signal as a function of coherence time at λ_{probe} = 616 nm and T_p = 250 fs for $\Delta\phi = 0$ (blue) and $\Delta\phi = \pi$ (red). Subtraction of the signals corresponding to $\Delta\phi = 0$ and $\Delta\phi = \pi$ enhances the amplitude of the desired 2D signal while eliminating the background (black).

function of t_{coh} for $\Delta\phi = 0$ and $\Delta\phi = \pi$ at a probe wavelength of 616 nm and T_p = 250 fs. Changing $\Delta\phi$ by π changes the phase of the desired oscillatory signal by π as well, while the background remains unchanged (red and blue curves). The subtracted signal is shown as the black curve in Figure 4. This phase-cycling procedure enhances the amplitude of the desired signal while simultaneously eliminating the background that does not depend of $\Delta\phi$.

To obtain the absorptive 2D spectrum, we acquire data as a function of t_{coh} at fixed T_p for $\Delta\phi = 0$ and $\Delta\phi = \pi$. Because we spectrally resolve the heterodyned signal using a spectrometer and CCD, the signal is collected in the frequency domain; that is, the detected signal can be written as $S(t_{coh}, T_p, \lambda_3; \Delta\phi)$. The first step is to obtain the background-free signal, $S(t_{coh}, T_p, \lambda_3) = S(t_{coh}, T_p, \lambda_3; 0) - S(t_{coh}, T_p, \lambda_3; \pi)$. We then perform a Jacobian transformation to obtain the data as a function of frequency ν_3, followed by interpolation to get equally spaced intervals along ν_3, which gives us $S(t_{coh}, T_p, f_3)$. We further subject our data to symmetry and causality conditions, as proposed by Ogilvie and coworkers.[12] Because the first two pulses are essentially interchangeable, the data must be symmetric with respect to $t_{coh} = 0$, or, in other words, the Fourier transform of $S(t_{coh}, T_p, f_3)$ along t_{coh} must be purely real. We enforce this symmetry condition by selecting the real part of the Fourier transform of $S(t_{coh}, T_p, f_3)$ (i.e., $\mathrm{Re}[S(f_1, T_p, f_3)]$) and inverse Fourier transforming it to obtain $S(\tau_{coh}, T_p, f_3)$ which is symmetric with respect to $\tau_{coh} = 0$. Next, we inverse Fourier transform this signal along f_3 to obtain $S(\tau_{coh}, T_p, t_3)$. Because no signal is emitted at negative t_3, that is, if the probe pulse interacts with the sample before the pump pulse, $S(\tau_{coh}, T_p, t_3) = 0$ for $t_3 < 0$. We apply this causality condition by multiplying $S(\tau_{coh}, T_p, t_3)$ with the Heaviside step function $\Theta(t_3)$. Finally, Fourier transforming the resulting signal along both τ_{coh} and t_3 gives us the complex absorptive 2D spectrum $S(\nu_1, T_p, \nu_3)$. This analysis procedure can be summarized as:

$S(t_{coh}, T_p, \lambda_3) \rightarrow S(t_{coh}, T_p, f_3)$	Jacobian transformation
$S(t_{coh}, T_p, f_3) \rightarrow S(f_1, T_p, f_3)$	Fourier transform along t_{coh}
$S(f_1, T_p, f_3) \rightarrow S(t_1, T_p, f_3)$	Inverse Fourier transform of $\mathrm{Re}[S(f_1, T_p, f_3)]$ along f_1
$S(t_1, T_p, f_3) \rightarrow S(t_1, T_p, t_3)$	Inverse Fourier transform along f_3
$S(t_1, T_p, t_3) \rightarrow S(\nu_1, T_p, \nu_3)$	Fourier transform of $\Theta(t_3) \times S(t_1, T_p, t_3)$ along t_1 and t_3

Figure 5b–d shows the absorptive 2D spectrum obtained using the above analysis at T_p = 500 fs. The horizontal axis

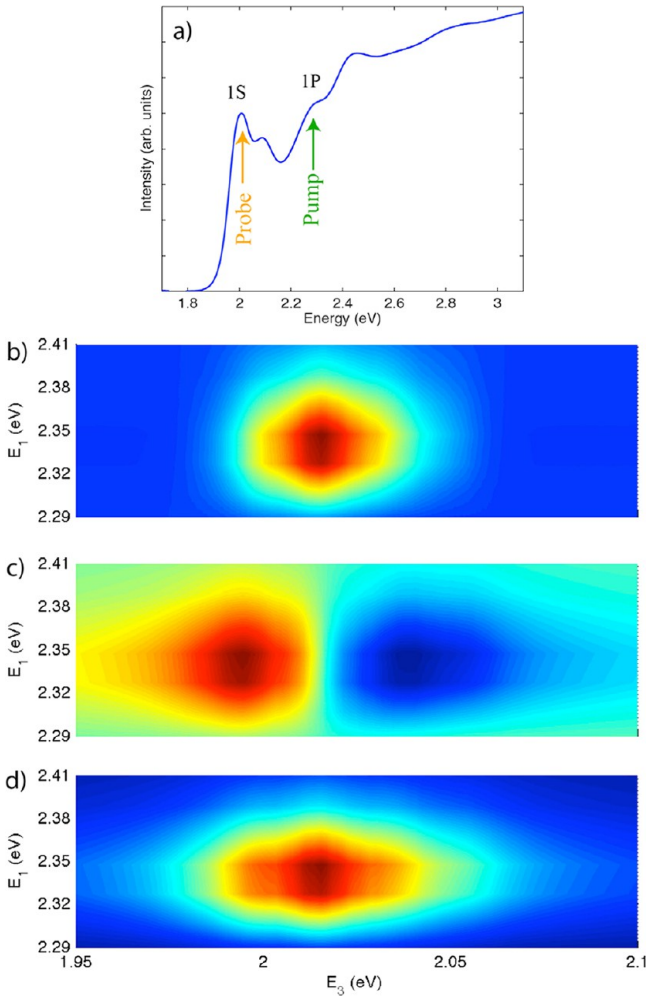

Figure 5. (a) Linear absorption spectrum of CdSe QDs. The arrows indicate the pump and probe pulse energies. (b) Real, (c) imaginary, and (d) absolute parts of the 2D absorptive spectrum of CdSe QDs at T_p = 500 fs.

corresponds to the emission axis obtained by Fourier transformation with respect to t_3, and the vertical axis, corresponding to excitation, is obtained by Fourier transformation along the t_{coh} axis. The two-color approach measures the coupling between different excitonic transitions, which in this case are 1P and 1S excitons (Figure 5a). The real part of the 2D spectrum has an absorptive line shape, whereas the imaginary part is dispersive in character. The population time dependence of the 2D spectrum is shown in Figure 6. The peak at (E_1, E_3) = (2.340, 2.015 eV) broadens and decreases in intensity with increasing T_p, which is indicative of population

dx.doi.org/10.1021/jp400603r | J. Phys. Chem. A 2013, 117, 6264–6269

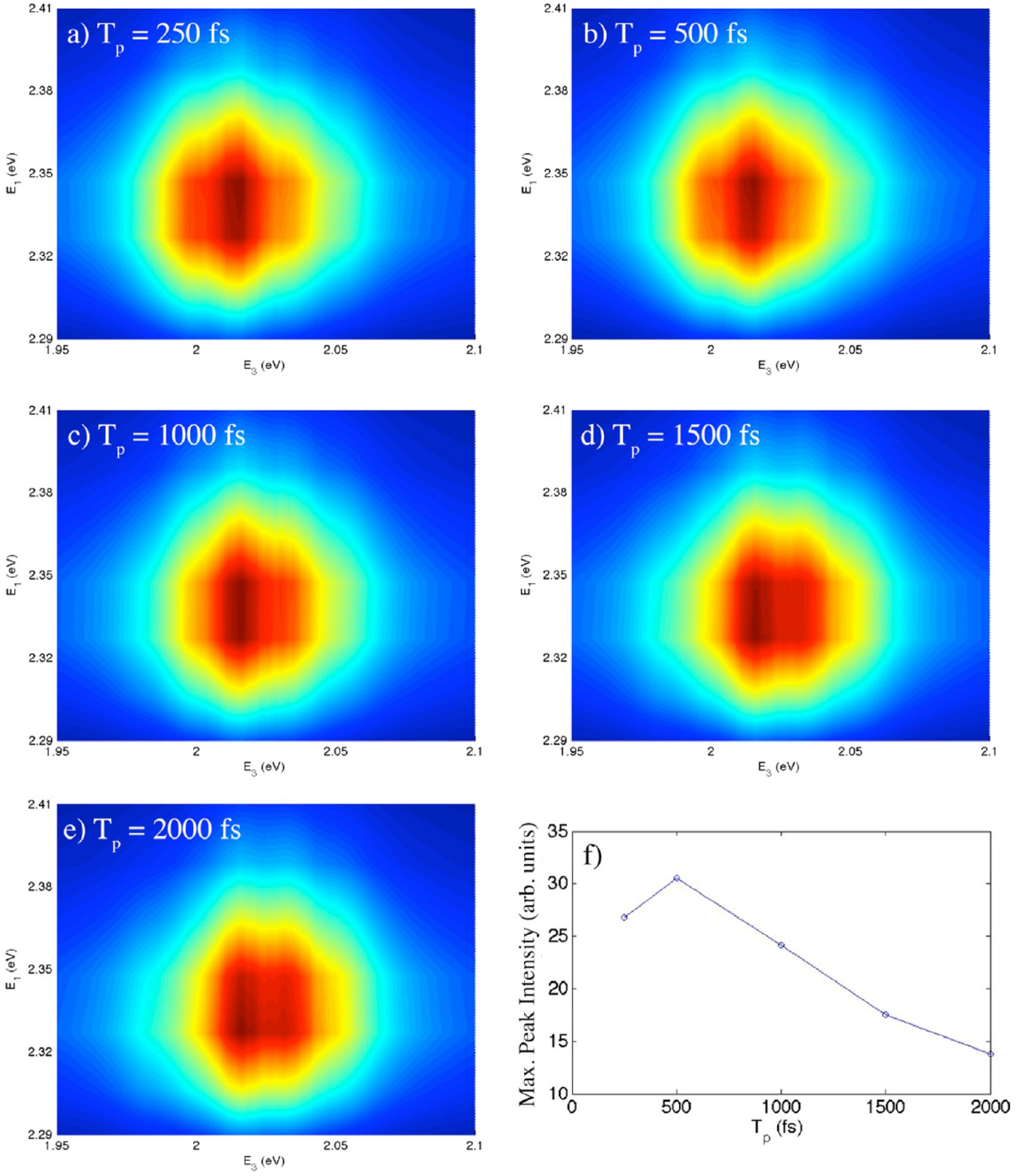

Figure 6. (a–e) Absolute part of 2D absorptive spectra for CdSe quantum dots for T_p = 250, 500, 1000, 1500, and 2000 fs. (f) Maximum intensity of the peak at (E_1, E_3) = (2.340, 2.015 eV) as a function of population time.

relaxation. Whereas these 2D spectra are shown merely to demonstrate the functionality of the dual-shaper setup, we note that the observed line shape and population relaxation are consistent with previous measurements.[20] The 2D measurements presented here do not utilize the polarization control capabilities of our setup. A comprehensive analysis of polarization-dependent signals will be presented in a subsequent paper. In pump–probe geometry, one can further extract R and NR signals from the measured 2D spectrum by employing three-step phase-cycling schemes,[12,21,22] whereas a fully collinear geometry requires at least a ten-step phase-cycling procedure to extract desired signals.[9,23]

In conclusion, we have demonstrated a dual-shaper setup with active phase stabilization. This configuration maintains excellent phase stability between the two pulse shapers, thereby extending the application of AOPDFs to 2Q measurements. The setup further allows us to independently control the polarization of individual shaped pulses. Previously, 2D

dx.doi.org/10.1021/jp400603r | J. Phys. Chem. A 2013, 117, 6264–6269

spectroscopy has been used to study many-body effects in quantum wells and excitonic fine-structure in QDs by mapping multiexcitonic interactions on a 2D plane.[4,20,24−29] By offering polarization control over individual shaped pulses, this dual-shaper setup further allows for the study of optical selection rules in QDs.

AUTHOR INFORMATION

Corresponding Author

*E-mail: pat.kambhampati@mcgill.ca. Tel: (514)-398-7228.

Author Contributions

§Pooja Tyagi and Jonathan I. Saari contributed equally.

Notes

The authors declare no competing financial interest.

ACKNOWLEDGMENTS

Financial support from the CFI, NSERC, FQRNT, and McGill University is gratefully acknowledged. We thank the McGill University Center for Self-Assembled Chemical Structures for use of their facilities.

REFERENCES

(1) Brixner, T.; Stenger, J.; Vaswani, H.; Cho, M.; Blankenship, R.; Fleming, G. Two-Dimensional Spectroscopy of Electronic Couplings in Photosynthesis. *Nature* **2005**, *434*, 625−628.

(2) Li, X.; Zhang, T.; Borca, C. N.; Cundiff, S. T. Many-Body Interactions in Semiconductors Probed by Optical Two-Dimensional Fourier Transform Spectroscopy. *Phys. Rev. Lett.* **2006**, *96*, 057406-1−057406-4.

(3) Shim, S.-H.; Strasfeld, D. B.; Ling, Y. L.; Zanni, M. T. Automated Two-Dimensional IR Spectroscopy Using a Mid-IR Pulse Shaper and Application of This Technology to the Human Islet Amyloid Polypeptide. *Proc. Natl. Acad. Sci. U.S.A.* **2007**, *104*, 14197−14202.

(4) Stone, K. W.; Gundogdu, K.; Turner, D. B.; Li, X.; Cundiff, S. T.; Nelson, K. A. Two-Quantum 2d FT Electronic Spectroscopy of Biexcitons in GaAs Quantum Wells. *Science* **2009**, *324*, 1169−1173.

(5) Myers, J. A.; Lewis, K. L. M.; Fuller, F. D.; Tekavec, P. F.; Yocum, C. F.; Ogilvie, J. P. Two-Dimensional Electronic Spectroscopy of the D1-D2-Cyt B559 Photosystem II Reaction Center Complex. *J. Phys. Chem. Lett.* **2010**, *1*, 2774−2780.

(6) Engel, G. S.; Calhoun, T. R.; Read, E. L.; Ahn, T.-K.; Mancal, T.; Cheng, Y.-C.; Blankenship, R. E.; Fleming, G. R. Evidence for Wavelike Energy Transfer through Quantum Coherence in Photosynthetic Systems. *Nature* **2007**, *446*, 782−786.

(7) Vaughan, J. C.; Hornung, T.; Stone, K. W.; Nelson, K. A. Coherently Controlled Ultrafast Four-Wave Mixing Spectroscopy. *J. Phys. Chem. A* **2007**, *111*, 4873−4883.

(8) Gundogdu, K.; Stone, K. W.; Turner, D. B.; Nelson, K. A. Multidimensional Coherent Spectroscopy Made Easy. *Chem. Phys.* **2007**, *341*, 89−94.

(9) Tian, P.; Keusters, D.; Suzaki, Y.; Warren, W. S. Femtosecond Phase-Coherent Two-Dimensional Spectroscopy. *Science* **2003**, *300*, 1553−1555.

(10) Wagner, W.; Li, C.; Semmlow, J.; Warren, W. S. Rapid Phase-Cycled Two-Dimensional Optical Spectroscopy in Fluorescence and Transmission Mode. *Opt. Express* **2005**, *13*, 3697−3706.

(11) Grumstrup, E. M.; Shim, S.-H.; Montgomery Matthew, A.; Damrauer Niels, H.; Zanni Martin, T. Facile Collection of Two-Dimensional Electronic Spectra Using Femtosecond Pulse-Shaping Technology. *Opt. Express* **2007**, *15*, 16681−16689.

(12) Myers, J. A.; Lewis, K. L. M.; Tekavec, P. F.; Ogilvie, J. P. Two-Color Two-Dimensional Fourier Transform Electronic Spectroscopy with a Pulse-Shaper. *Opt. Express* **2008**, *16*, 17420−17428.

(13) DeFlores, L. P.; Nicodemus, R. A.; Tokmakoff, A. Two-Dimensional Fourier Transform Spectroscopy in the Pump−Probe Geometry. *Opt. Lett.* **2007**, *32*, 2966−2968.

(14) Tekavec, P. E.; Myers, J. A.; Lewis, K. L. M.; Ogilvie, J. P. Two-Dimensional Electronic Spectroscopy with a Continuum Probe. *Opt. Lett.* **2009**, *34*, 1390−1392.

(15) Xiong, W.; Zanni, M. T. Signal Enhancement and Background Cancellation in Collinear Two-Dimensional Spectroscopies. *Opt. Lett.* **2008**, *33*, 1371−1373.

(16) Middleton, C. T.; Strasfeld, D. B.; Zanni, M. T. Polarization Shaping in the Mid-IR and Polarization-Based Balanced Heterodyne Detection with Application to 2D IR Spectroscopy. *Opt. Express* **2009**, *17*, 14526−14533.

(17) Shim, S. H.; Strasfeld, D. B.; Ling, Y. L.; Zanni, M. T. Automated 2d IR Spectroscopy Using a Mid-IR Pulse Shaper and Application of This Technology to the Human Islet Amyloid Polypeptide. *Proc. Natl. Acad. Sci. U.S.A.* **2007**, *104*, 14197−14202.

(18) Jonas, D. M Two-Dimensional Femtosecond Spectroscopy. *Annu. Rev. Phys. Chem.* **2003**, *54*, 425−463.

(19) Khalil, M.; Demirdöven, N.; Tokmakoff, A. Obtaining Absorptive Line Shapes in Two-Dimensional Infrared Vibrational Correlation Spectra. *Phys. Rev. Lett.* **2003**, *90*, 047401-1−047401-4.

(20) Turner, D. B.; Hassan, Y.; Scholes, G. D. Exciton Superposition States in CdSe Nanocrystals Measured Using Broadband Two-Dimensional Electronic Spectroscopy. *Nano Lett.* **2012**, *12*, 880−886.

(21) Zhang, Z. Y.; Wells, K. L.; Hyland, E. W. J.; Tan, H. S. Phase-Cycling Schemes for Pump-Probe Beam Geometry Two-Dimensional Electronic Spectroscopy. *Chem. Phys. Lett.* **2012**, *550*, 156−161.

(22) Yan, S. X.; Tan, H. S. Phase Cycling Schemes for Two-Dimensional Optical Spectroscopy with a Pump-Probe Beam Geometry. *Chem. Phys.* **2009**, *360*, 110−115.

(23) Tan, H. S. Theory and Phase-Cycling Scheme Selection Principles of Collinear Phase Coherent Multi-Dimensional Optical Spectroscopy. *J. Chem. Phys.* **2008**, *129*, 124501-1−124501-3.

(24) Harel, E.; Rupich, S. M.; Schaller, R. D.; Talapin, D. V.; Engel, G. S. Measurement of Electronic Splitting in Pbs Quantum Dots by Two-Dimensional Nonlinear Spectroscopy. *Phys. Rev. B* **2012**, *86*, 075412-1−075412-5.

(25) Yurs, L. A.; Block, S. B.; Pakoulev, A. V.; Selinsky, R. S.; Jin, S.; Wright, J. Multiresonant Coherent Multidimensional Electronic Spectroscopy of Colloidal PbSe Quantum Dots. *J. Phys. Chem. C* **2011**, *115*, 22833−22844.

(26) Wong, C. Y.; Scholes, G. D. Biexcitonic Fine Structure of CdSe Nanocrystals Probed by Polarization-Dependent Two-Dimensional Photon Echo Spectroscopy. *J. Phys. Chem. A* **2010**, *115*, 3797−3806.

(27) Wong, C. Y.; Scholes, G. D. Using Two-Dimensional Photon Echo Spectroscopy to Probe the Fine Structure of the Ground State Biexciton of CdSe Nanocrystals. *J. Lumin.* **2010**, *131*, 366−374.

(28) Stone, K. W.; Turner, D. B.; Gundogdu, K.; Cundiff, S. T.; Nelson, K. A. Exciton Correlations Revealed by Two-Quantum, Two-Dimensional Fourier Transform Optical Spectroscopy. *Acc. Chem. Res.* **2009**, *42*, 1452−1461.

(29) Turner, D. B.; Nelson, K. A. Coherent Measurements of High-Order Electronic Correlations in Quantum Wells. *Nature* **2010**, *466*, 1089−1092.